A MEMS transducer for detection of acoustic emission events

D. Ozevin and S.P. Pessiki
Department of Civil and Environmental Engineering
Lehigh University, Bethlehem, PA, USA

D.W. Greve and I.J. Oppenheim
Department of Civil and Environmental Engineering,
Carnegie Mellon University, Pittsburgh, PA, USA

***Abstract*—Acoustic emissions are ultrasonic pulses produced in solids when irreversible damage occurs under mechanical loading. We report on the design and testing of a MEMS device, adapted from cMUT technology, to detect acoustic emissions. The device is fabricated in a surface-machined MEMS process and consists of diaphragms supported by springs above a plate. When a DC bias voltage is applied, vibration of the spring-supported diaphragm causes a time-varying current. The MEMS device contains seven independent transducers with resonant frequencies in the range of 100 kHz to 1 MHz. The availability of multiple signals allows for redundant sensing and may facilitate distinction of true acoustic emissions from other events. We report the detection of actual acoustic emission events in structural testing, comparing the performance of the MEMS device with a conventional PZT acoustic emission transducer. In the test, a MEMS device and a conventional transducer were attached to a steel beam specimen which was loaded to failure. Strong acoustic emission events were simultaneously detected by both types of transducers.**

Keywords-acoustic emission; capacitive, MEMS.

I. INTRODUCTION

Acoustic emission sensing is an important technology for managing critical civil infrastructure components such as steel highway and railway bridges. These structures develop fatigue cracks with repeated loading, and require periodic inspection to monitor the progress of those cracks and, accordingly, to determine when repair or replacement is required. As many of the cracks are stable, only a subset experience ongoing crack growth; acoustic emission sensing is increasingly used to distinguish between inactive and active cracks.

Acoustic emissions are transient ultrasonic waves released from microscopic zones, such as a crack tip, during irreversible damage, such as crack extension; therefore, acoustic emissions constitute evidence that a crack is active. However, impacts and friction effects also produce stress waves, and therefore it is necessary to discriminate true acoustic emissions from spurious events. Localization of the signal source is one key discriminant, and waveform characteristics constitute another.

Most of the emitted energy is observed at frequencies between 100 kHz and 1 MHz. Commercial acoustic emission transducers may be either resonant or broadband, and generally employ a piezoceramic element to sense motion normal to the surface of the steel member; the transducers are fluid-coupled to the steel with a thin grease layer, and therefore constitute single-channel, single-mode detectors.

We describe a resonant, capacitive MEMS-based transducer for acoustic emission detection, adapted from our earlier development of a MEMS ultrasonic transducer [2]. It is intended that the arrival of the acoustic emission transient will set the transducer diaphragm into vibration. In the long term, we envision the MEMS-based transducer being integrated with data-processing electronics. In this paper we show that we can fabricate multiple resonant transducers on one chip, each transducer with multiple vibration modes. The multiple transducers, and multiple modes, can be used to detect acoustic emission energy at several different frequencies, and this additional information may provide a better understanding of the damage processes and should help discriminate between mechanical noise and true acoustic emission events.

II. TRANSDUCER DESIGN

Figure 1 compares the MEMS transducer with a conventional piezoceramic acoustic emission transducer [3]. In the conventional transducer, ultrasonic vibrations of the transmitting medium are coupled to a PZT element, causing a terminal voltage $v(t)$ proportional to the strain. The backing material is chosen to provide the appropriate amount of damping for the desired transducer bandwidth. In the MEMS transducer, ultrasonic vibrations are coupled to the bottom plate of a capacitive transducer. Vibrations of the top plate with respect to the bottom plate produce current $i(t) = V_{DC}(dC/dt)$ in the external circuit, where V_{DC} is the DC bias voltage and C is the capacitance. In this case the peak frequency is $\omega_0 = \sqrt{k/m}$, where k is the effective spring constant and m is the effective mass of the top plate. The bandwidth is governed by squeeze-film damping and emission of energy into the air [4], which is determined by the size and spacing of the etch release holes.

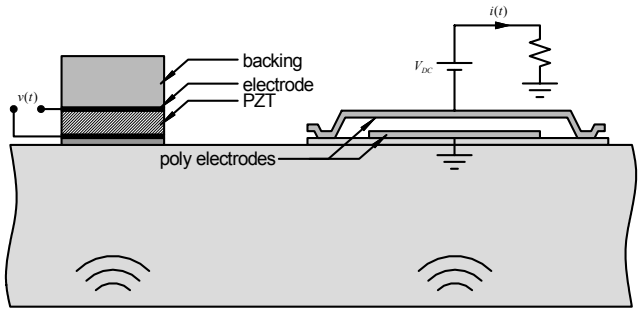

Figure 1. Conventional piezoelectric (left) and MEMS (right) transducers for acoustic emission. (not drawn to the same scale).

The devices used in this work were fabricated in the multi-user MUMPS process. This process has three polysilicon structural layers, and in this work the plates are formed by the POLY0 and POLY1 layers. The top plate (diaphragm) is 2.0 μm in thickness, the gap between the two plates is 1.25 μm, and the chip is 1 cm square, containing seven transducers at different resonant frequencies.

To build a transducer with the relatively low resonant frequencies needed, we support a polysilicon sheet by a set of cross-shaped springs, as shown in Figure 2. Considering each sheet a rigid body, it has a translational mode and two rocking modes; because of symmetry in this particular design, the two rocking modes have the same frequency. To achieve a design target of moderate underdamped response, we use an appropriate etch hole spacing.

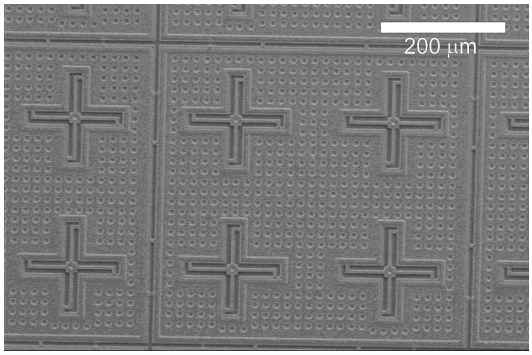

Figure 2. Scanning electron micrograph showing top plate; the cross-shaped springs and etch release holes are visible.

The CAD layout drawing of the chip is shown in Figure 3. (We label elements in four rows, A-D, and three columns, 1-3; elements B3, C1-C3, and D1-D3 comprise the seven acoustic emission transducers; elements A2, B1, and B2 are other test structures fabricated on the chip.) For testing, the chip is attached with silver epoxy to a 64-pin ceramic package and wire-bonded.

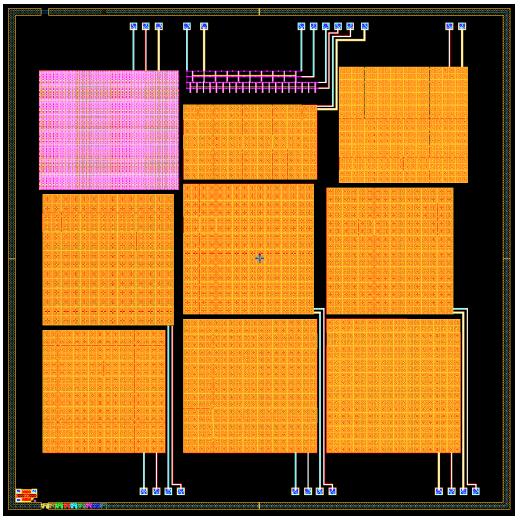

Figure 3. CAD layout of the chip. (D1 in lower left corner)

Table I summarizes the characteristics of the seven different transducers. In this table, n is the number of individual elements connected in parallel; L_1 and L_2 are the length of the short and long spring segments, respectively; L_m is the size of each element, and A is the total area of the transducer. The resonant frequencies, measured in vacuum, are f_1 and f_2.

Table I. Characteristics of MEMS transducers.

	C1	C2	C3	D1	D2	D3	B3
n	49	64	64	64	81	100	90
L_1 [μm]	8	8	8	8	8	8	8
L_2 [μm]	45	40	33	27	22	19	12
L_m [μm]	380	330	320	310	300	270	240
A [mm^2]	7.23	7.16	6.73	6.32	7.51	7.53	6.29
f_1 [kHz]	107	150	178	187	210	272	-
f_2 [kHz]	150	207	252	275	317	405	925

The resonant frequency and damping of transducers can be determined from admittance measurements with an applied DC bias. A value of 2.5 has been extracted for Q (at atmospheric pressure) in the lowest mode of the D2 transducer, representative of the design target for moderate underdamping.

III. Structural Testing

In our earlier work, the MEMS device was mounted on a steel plate and excited by pencil lead breaks, which are used in practice to simulate, physically, an acoustic emission event. Those results [5] show that the transducer responds both in a translational mode and in a rocking mode, and that two distinct wave speeds are detected, corresponding to the symmetric and antisymmetric Lamb wave modes. The multimode response, and the presence of multiple transducers on the chip, provided more waveform information than is regularly obtained from a conventional transducer, and provided additional data with which to localize the source.

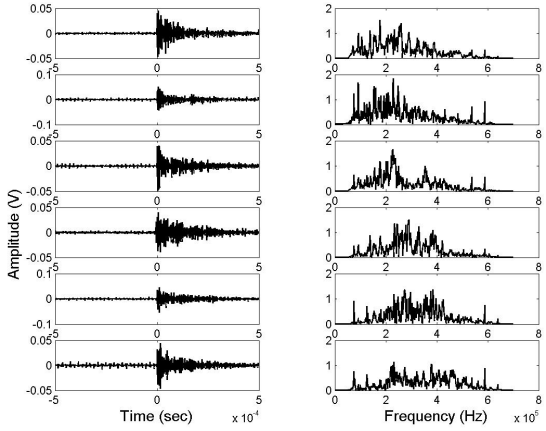

Figure 4. Signals obtained at six transducers in pencil lead break experiment; top-to-bottom: transducers C1, C2, C3, D1, D2, and D3

Figure 4 shows the signals, and their transform into the frequency domain, from six transducers when the device was subjected to a pencil break 2 cm distant. The tests were performed with a DC bias voltage of 9 V, and 60 kHz – 600 kHz band-pass Butterworth filtering was applied.

Detection of true acoustic emissions by the MEMS device was demonstrated in laboratory testing of a steel member loaded in bending. We sought to study propagation of cracking in weld metal, and therefore fabricated a test specimen from two segments of A50 steel joined at midspan by a full zone of weld metal, and a precrack was induced in the weld zone. The specimen was 76.2 cm long, 54 mm high and 25 mm wide, with the crack extending 6 mm into the specimen.

The test setup is depicted in Figure 5. A conventional PZT transducer (Physical Acoustics Corporation, model R30) was mounted to the left and the MEMS device was mounted to the right of midspan; our objective was to compare the detection capability achieved by transducers on the MEMS device with a "ground truth" obtained from the conventional transducer. Signals were collected from five different MEMS transducers on the device, along with the signal from the conventional transducer; the MEMS transducers were biased with a DC voltage of 9 V. After amplification, two channels were digitized by a National Instruments 5122 DAQ board and four channels were digitized by a Tektronix TDS2014 oscilloscope. Labview programs were used to control the testing machine and data acquisition. The trigger signals for the oscilloscope and DAQ board were taken from the conventional transducer. After each trigger event, records were written to hard disk under computer control. The testing machine load and displacement were also recorded as a function of time for correlation with the acoustic emission records. Five nominally identical specimens were tested to failure.

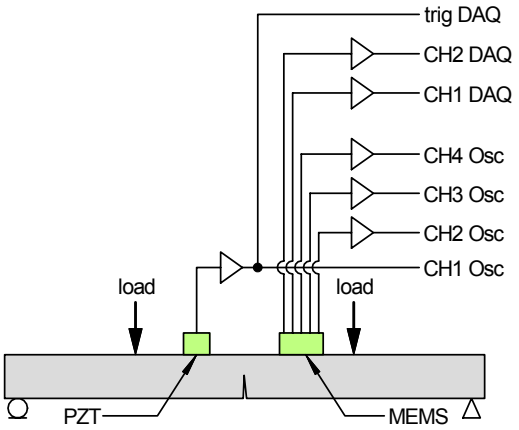

Figure 5. Experimental arrangement for transducer testing.

The tests were conducted on an Instron 4400 universal testing machine, advancing the machine crosshead to produce a monotonic increase in structural displacement (deflection) while measuring the force applied to the test specimen by the crosshead. The specimen is supported at its two ends while the crosshead (through a spreader beam) delivers the test load to two points symmetric about the center of the span; this test condition is termed a "four-point" loading which creates a zone of constant internal bending moment between the load points. During the several seconds required to write the records to disk after each triggering event, no new data could be acquired, and consequently it is possible that closely-spaced acoustic emission events could be missed. In order to minimize that possibility, a slow crosshead speed of 0.025 mm/min was used.

Structural test results are regularly represented by plotting the applied load against the displacement, as shown in Figure 6 for one representative experiment. A linear region within a load-displacement plot reflects linear elastic response. The slight initial stiffening seen in Figure 6, as the load increases to roughly 5 kN, is explained by compression of elastomeric layers that were used at the supports and the loading points to prevent coupling of mechanical noise during testing. The specimen itself displays linearly elastic behavior, interpreted as damage-free, until the displacement approaches 5 mm and the load approaches 20 kN. As the displacement increases further, the specimen displays a softening response which is associated with damage (and nonrecoverable deformation) produced by plasticity and crack extension. At a displacement near 6.3 mm the load dropped abruptly from 23.5 kN to 15 kN because the crack became unstable and underwent gross extension; had the structure been subjected to a constant load of 23.5 kN, collapse would have occurred. The specimen then displays dramatic softening as the displacement increases from 6.3 to 17.5 mm, followed by another abrupt load drop from 10 kN to 2.5 kN, at which point the experiment was terminated.

Acoustic emission events detected by the conventional transducer are indicated in Figure 6 by red circles. As expected, events are observed throughout the segments of the load-displacement plot where softening (damage) is observed. Note that an appreciable number of events are observed prior to the first load drop. Detection of these events represents a major objective of acoustic emission testing, as these events indicate that the member is sustaining damage and crack growth.

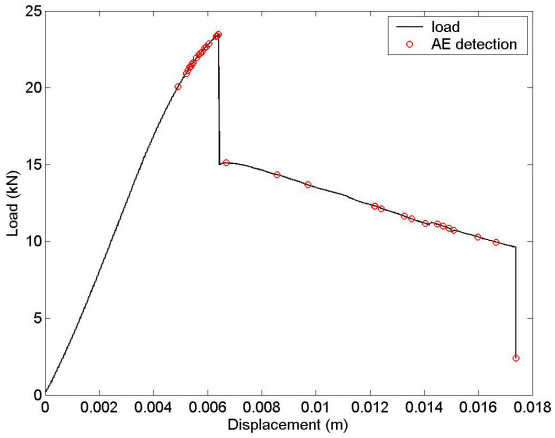

Figure 6. Load-displacement characteristic with acoustic emission events detected by the conventional transducer indicated as circles.

We next compare the acoustic emission events detected by the conventional and by the MEMS transducers. Figure 7 compares the signal from one MEMS transducer with the signal from the conventional transducer for one acoustic emission event that occurred at a load of 21.3 kN. Both transducers unambiguously detect the acoustic emission event, but the conventional transducer displays a larger signal level and better signal to noise ratio. The lower signal level of the MEMS transducer is a consequence of the generally superior value for the transformer ratio n for piezoelectric transducers. (The transformer ratio $n = -i/u$ is the ratio between the output

electrical current *i* and the wave velocity *u*). The higher noise level in the MEMS transducer is in part due to electrical interference in the arrangement used for this work.

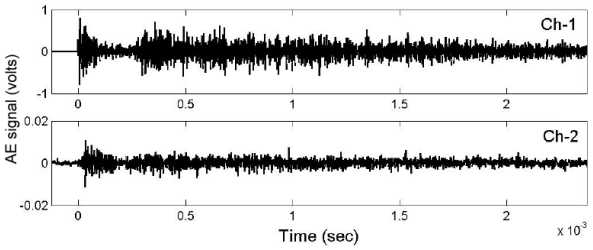

Figure 7. Comparison of signals detected by the piezoelectric transducer (top trace) and the MEMS transducer (bottom trace) at 21.3 kN.

Because of the lower signal-to-noise ratio, not all acoustic emission events detected with the conventional transducer were detected by the MEMS transducer. Figure 8 compares the signal levels and the detected events for the two types of transducers. A total of 33 events were detected by the conventional transducer. The left-hand plot records the maximum signal level during the event; signals ranged from tenths of a volt to above one volt, which was the saturation limit of the oscilloscope. The right-hand plot shows the maximum signal level recorded by the C2 MEMS transducer during the 33 detected acoustic emission events. Some events did not give a clear signal above the noise for the MEMS transducer, and are indicated with open points. A significant proportion of the events, roughly 40%, were successfully detected by the MEMS transducers, including a number of events prior to the load drop at 23.5 kN. This experiment shows that the MEMS transducer is sufficiently sensitive at present to detect acoustic events indicative of damage and crack growth.

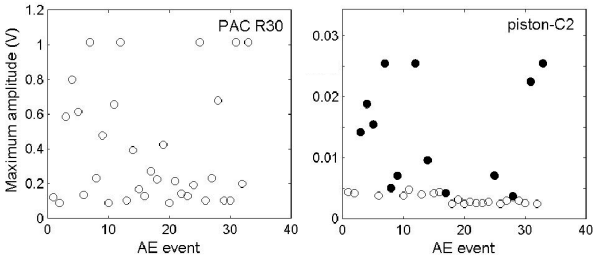

Figure 8. Comparison of MEMS and piezoelectric transducers for 33 events.

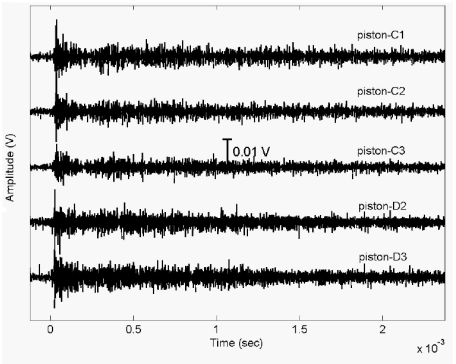

Figure 9. Signals detected by five different MEMS transducers at 21.1 kN.

MEMS transducers offer the possibility of simultaneous detection by multiple redundant transducers and/or detection by transducers with different resonant frequencies. This may make it possible to discriminate between real and spurious signals. Simultaneous detection by five different transducers is shown in Figure 9 for an acoustic emission event that occurred at a load of 21.1 kN, prior to the first load drop, and this event is clearly detected by all five MEMS transducers.

IV. SUMMARY

We have developed capacitive MEMS transducers capable of detecting acoustic emission signals. The resonant frequency of each transducer is determined by the spring constant and the effective mass of the supported diaphragm. In order to act as a resonant type transducer, set into vibration by an acoustic emission stress wave, moderate underdamping is desired. This has been achieved by appropriate choice of the spacing of etch release holes.

In this work we have demonstrated the detection of acoustic emission events that signal damage and crack growth in a structural member. However, not all the acoustic emission events detected by a conventional piezoelectric transducer were detected by the MEMS transducer. This is a consequence of the somewhat worse signal-to-noise ratio of the MEMS transducer, in part as a result of electrical interference. We believe that the signal-to-noise ratio can be improved with better packaging and shielding.

ACKNOWLEDGMENT

We thank the Pennsylvania Infrastructure Technology Alliance, and we thank the National Science Foundation for support under Grant No. CMS-0329880. Any opinions, findings, and conclusions or recommendations expressed in this material are those of the authors and do not necessarily reflect the views of the National Science Foundation.

REFERENCES

[1] Stephens, R.W., and Pollock, A.A., "Waveforms and Frequency Spectra of Acoustic Emission," Journal of the Acoustical Society of America, Vol. 50, No. 3, 1971, pp. 904-910.

[2] X. Jin, O. Oralkan, F.L. Degertekin, and B.T. Khuri-Yakub, "Characterization of one-dimensional capacitive micromachined ultrasonic immersion transducer arrays," *IEEE Transactions on Ultrasonics, Ferroelectrics, and Frequency Control*, vol. 48, pp. 750-760 (2001).

[3] Gautschi, G., Piezoelectric Sensorics, Springer-Verlag, 2001, 1st Edition.

[4] Oppenheim, I.J., Jain, A., and Greve, D.W., "Electrical Characterization of Coupled and Uncoupled MEMS Ultrasonic Transducers," IEEE Transactions on Ultrasonics, Ferroelectrics, and Frequency Control, Vol. 50, No. 3, March 2003, pp. 297-304.

[5] Ozevin, D., Greve. D. W., Oppenheim, I. J., and Pessiki, S. P., "Steel Plate Coupled Behavior of MEMS Transducer Developed for Acoustic Emission Testing," *26th European Conference on Acoustic Emission Testing*, Berlin, September 2004.